molecular pharmaceutics

Article

pubs.acs.org/molecularpharmaceutics

Electrospun Fibers with Plasmid bFGF Polyplex Loadings Promote Skin Wound Healing in Diabetic Rats

Ye Yang,[†,‡] Tian Xia,[§] Fang Chen,[†] Wei Wei,[§] Chaoyu Liu,[†] Shuhui He,[†] and Xiaohong Li*[,†]

[†]Key Laboratory of Advanced Technologies of Materials, Ministry of Education of China, School of Materials Science and Engineering, Southwest Jiaotong University, Chengdu 610031, P. R. China

[‡]School of Pharmacy, Anhui University of Traditional Chinese Medicine, Hefei 230031, P. R. China

[§]Department of Pathology, The 452nd Hospital of People's Liberation Army, Chengdu 610021, P. R. China

ABSTRACT: Deep or chronic skin wounds are difficult to heal spontaneously due to the lack of scaffold to guide cell growth and reduced levels and activities of endogenous growth factors. Emulsion electrospinning process integrated with DNA condensation techniques indicated potentials to gradually release DNA, but no attempt has been made to clarify the advantages in promoting tissue regeneration and wound recovery. In this study, polyplexes of basic fibroblast growth factor-encoding plasmid (pbFGF) with poly(ethylene imine) were incorporated into electrospun fibers with a core–sheath structure, and poly(ethylene glycol) was included into the fiber sheath to allow a sustained release of pbFGF for 4 weeks. *In vitro* tests on mouse embryo fibroblasts indicated that pbFGF-loaded fibrous mats enhanced cell proliferation by the autocrine bFGF, and an effective cell transfection proceeded for over 28 days. Skin wounds were created in the dorsal area of diabetic rats for *in vivo* evaluation of skin regeneration after being covered with pbFGF-loaded fibrous mats. The gradual pbFGF release revealed significantly higher wound recovery rate with improved vascularization, enhanced collagen deposition and maturation, complete re-epithelialization and formation of skin appendages. The above results demonstrate the potential use of pbFGF-loaded electrospun fibrous mats to accelerate the healing of skin ulcers for patients with diabetic mellitus.

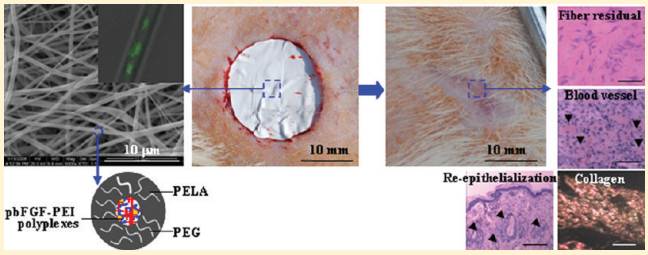

KEYWORDS: *emulsion electrospinning, core–sheath structure, pbFGF polyplex-loaded fibers, diabetic ulcer, skin regeneration*

INTRODUCTION

The prevalence of diabetes has increased tremendously worldwide, and diabetic complications have become a serious issue for public health. One of these complications is diabetic skin ulcer, which is responsible for more hospitalizations than any other complications. Most skin wounds with minor epidermal injury can regenerate themselves; however, when the injury is severe, such as full-thickness loss, or results from chronic ulcer, the skin loss cannot regenerate spontaneously.[1] Levels of endogenous growth factors (GFs) in chronic wounds are too low to promote angiogenesis and wound repair. Topical application of GFs and GF-containing gels has been explored as a possibility to improve the wound recovery.[2] But the weakness of exogenous delivery includes short half-life and quick release, leading to mild improvement without dose-dependent therapeutic effects.[3] Therefore, prolongation, stabilization and localization of the bioactivity over an extended time period are required to apply GFs practically in wound repair.

Polymeric fibrous scaffolds have been widely used in tissue engineering due to their desirable properties of extracellular matrix (ECM)-like architecture, large surface-to-volume ratio to allow efficient cell attachment, high porosity and interconnected pores to enable free access of oxygen and nutrient supplies for cell growth.[4] With the availability of surface modification and flexibility in choosing matrix materials, GFs have been integrated into electrospun fibers through physical adsorption or grafting, blend electrospinning or coaxial electrospinning.[5,6] Emulsion electrospinning was developed in our previous work to maintain the structural integrity and bioactivity of the sensitive protein incorporated into electrospun fibers.[7] *In vivo* evaluation of skin regeneration indicated that GF-loaded electrospun fibers revealed significantly higher wound recovery rate compared with fibrous mats infiltrated with free GFs.[8] However, controllable release with bioactivity preservation during a long period represents a major challenge for GF-loaded fibrous scaffolds.[9] The denaturation related to storage or scaffold formulation and the high price of purified GFs are additional restrictive factors of the application into inductive tissue engineering scaffolds. Therefore, loading of functional genes in fibers is an alternative strategy to extend periods of gene availability and thus protein expression to times similar to the release of GFs from fibrous scaffolds.

Several strategies have been proposed to incorporate plasmid DNA (pDNA) into electrospun ultrafine fibers. Luu et al. initially fabricated synthetic polymer/DNA composite scaffolds

Received: May 10, 2011
Revised: September 14, 2011
Accepted: November 17, 2011
Published: November 17, 2011

through blend electrospinning, and DNA was found localizing on the fiber surface rather than becoming encapsulated within fibers, resulting in a large initial burst release of over 20% during 15 min and low transfection efficiency.[10] To induce sufficient protein production pDNA was incorporated into electrospun fibers through electrostatic layer-by-layer deposition of polycations and pDNA,[11] or including polycations into the sheath of coaxial electrospun fibers.[12] But the depletion of polycations from fibers, which should be stronger under *in vivo* conditions, causes only partial condensation with the released pDNA and undesirable side effects of polycations. Alternatively, pDNA was condensed into nanoparticles before being absorbed onto or entrapped into electrospun fibers. Nie et al. prepared electrospun fibers with surface deposition of pDNA/chitosan nanoparticles, indicating high cytotoxicity and short-term gene expression due to the significant initial release of pDNA nanoparticles.[13] Liang et al. embedded pDNA nanoparticle into fibers through blend electrospinning, showing an extremely low transfection efficiency of less than 1% due to a limited release of pDNA from fibrous scaffolds.[14] In our previous study polyethylene glycol (PEG) was added into the fiber sheath to modulate the release of pDNA polyplexes from core−sheath fibers. The effective release lifetime can be controlled between 6 and 25 days, dependent on the loading amount and molecular weight of PEG.[15]

Electrospun core−sheath fibers integrated with DNA condensation techniques indicate potentials to gradually release DNA for manipulating desired signals at effective levels within the local tissue microenvironment. But no attempt has been made to clarify the advantages in promoting tissue regeneration and wound recovery. It was indicated that the levels of basic fibroblast growth factor (bFGF) are insufficient in chronic wounds,[16] resulting in difficulties in healing skin ulcers in patients with diabetes mellitus. Polyplexes of bFGF-encoding plasmid (pbFGF) and poly(ethylene imine) (PEI) were encapsulated into emulsion electrospun poly(DL-lactide)-poly(ethylene glycol) (PELA) fibers with a core−sheath structure, mimicking viruses whose protein shells sealed the compact DNA molecules inside a compartment.[17] PEG was included to modulate the release of pbFGF polyplexes to cover the wound healing process, and the capabilities to enhance the target protein expression and cell growth were determined on mouse embryo fibroblasts (MEFs) *in vitro*. Skin wounds were created in the dorsal area of diabetic rats for *in vivo* evaluation of skin regeneration after being covered with pbFGF polyplex-loaded fibrous mats.

EXPERIMENTAL SECTION

Materials. The pbFGF (6777 bp), encoding fusion protein of recombinant murine bFGF/enhanced green fluorescent protein (bFGF/eGFP) within a cytomegalovirus promoter (C-terminal eGFP-tagged protein), were from FulenGen Co. (Guangzhou, China). The plasmid was grown in *Escherichia coli* DH5α bacterial culture using LB growth media, purified using Qiagen Giga kit (Hilden, Germany), and stored in Tris−EDTA buffer (TE, 10 mM Tris-HCl, 1 mM EDTA, pH 8.0) at 4 °C. PELA (M_w = 42.3 kDa, M_w/M_n = 1.23) was prepared by bulk ring-opening polymerization of lactide/PEG using stannous chloride as initiator.[18] All the electrophoresis reagents, PEG (M_w = 2, 4 kDa), PEI (M_w = 25 kDa), 4′,6-diamidino-2-phenylindole (DAPI), bisbenzimide (Hoechst 33258), bovine serum albumin (BSA), streptozotocin (STZ), pentobarbital, HEPES buffer, sirius red (SR) were from Sigma−Aldrich (St. Louis, MO). Protein molecular weight marker and RIPA lysis buffer were from Beyotime Institute of Biotechnology (Shanghai, China). Rabbit anti-mouse antibodies of Collagen I, CD34, β-actin and proliferating cell nuclear antigen (PCNA), goat anti-rabbit IgG-horseradish peroxidase (HRP) and 3,3′-diaminobenzidine (DAB) developer were purchased from Biosynthesis Biotechnology Co. LTD (Beijing, China). Ultrapure water from a Milli-Q biocel purification system (UPI-IV-20, Shanghai UP Scientific Instrument Co., Ltd., Shanghai, China) was used. All other chemicals were analytical grade and received from Changzheng Regents Company (Chengdu, China) unless otherwise indicated.

Fabrication of Fibers with the Loading of pbFGF Polyplexes. Polyplexes of pbFGF and PEI were prepared in phosphate buffer solution (PBS), and emulsified into PELA solution in chloroform, followed by emulsion electrospinning as described elsewhere.[15] Briefly, 500 μL of PEI solution (22.3 mM in pH 7.0 PBS) and 500 μL of pbFGF solution (1 mg/mL in pH 7.0 PBS) were mixed together, vortexed for 30 s and centrifuged at 15000*g* for 30 min. The pellets were resuspended into 50 μL of pH 7.0 PBS, and emulsified into 3.0 mL of chloroform containing 450 mg of PELA and 50 mg of PEG. The resulting emulsion was added in a 5 mL syringe attached to a metal capillary, and a steady flow at 1.6 mL/h out of the capillary was controlled by a microinject pump (Zhejiang University Medical Instrument Co., Hangzhou, China). The electrospinning apparatus was equipped with a high-voltage Statitron (Tianjing High Voltage Power Supply Co., Tianjing, China), and the applied voltage was set as 20 kV. The collected fibers were lyophilized overnight to remove any solvent and water residues and stored at 4 °C. PEG with molecular weights of 2 and 4 kDa was used, and the obtained fibers were named as Fb2 and Fb4, respectively. Electrospun fibers without inoculation of pbFGF polyplex were also prepared as above, and named as Fa2 and Fa4, where the last number represents the molecular weight of PEG used.

In order to visualize the pbFGF distribution in fibers, pbFGF was labeled with DAPI through combination with the guanine and thymine nucleotides of DNA. Briefly, pbFGF was added into DAPI solution (10 μg/mL in 10 mM PBS), and the mixture was kept in the dark for 5 min before being dialyzed to remove any residual DAPI. Electrospun fibers loaded with labeled pbFGF polyplexes were prepared as above.

Characterization of Fibers with the Loading of pbFGF Polyplexes. The electrospun fibers were mounted on metal stubs by using conductive double-sided tape and sputter-coated with gold for a period up to 120 s. The morphologies were determined by use of a scanning electron microscope (SEM, FEI Quanta 200, The Netherlands) at an accelerating voltage of 20 kV. The fiber diameter was measured from the SEM images, and five images were used for each fiber sample. From each image, at least 20 different fibers and 100 different segments were randomly selected and their diameter measured to generate an average fiber diameter by using Photoshop v8.0.

The distribution of pbFGF in composite fibers was examined by a laser confocal scanning microscope (LCSM, Leica TCS SP2, Germany). The excitation and emission wavelengths of DAPI were set as 364 and 454 nm, respectively. In brief, all the parameters including the laser intensity and gain were adjusted until fluorescent signals could not be seen from the control sample, then without changing the settings, the same parameters were used to observe fiber samples. A superimposing of the fiber image without excitation on the same

fiber image with excitation provided a representation of the structure of the composite fibers.

Core loading of pbFGF in the ultrafine fibers was quantified with Hoechst 33258 dye, which can preferentially bind to guanine and thymine rich regions of pDNA. In brief, a known amount of fibers (ca. 50 mg) was dissolved in 500 μL of chloroform, and pbFGF encapsulated in fibers was extracted by PBS containing 10 mg/mL heparin. To determine the encapsulation efficiency, the extracted pbFGF was mixed with Hoechst 33258 and the fluorescence intensity was measured by a fluorospectrophotometer (Hitachi F-7000, Japan) at an excitation wavelength of 365 nm and an emission wavelength of 460 nm. The extraction efficiency was calibrated by adding a certain amount of pbFGF polyplexes into PELA-PEG/chloroform solution along with the same concentration as above and extracted using the above method. The pbFGF contents were determined in triplicate for at least three different batches.

Release Profiles of pbFGF from Electrospun Fibers. Electrospun fibrous mats with pbFGF polyplex inoculations were cut into small squares (1 × 1 cm^2) with a total mass of about 100 mg, and immersed in 3.0 mL of pH 7.4 PBS containing 10 mg/mL heparin. The suspensions were kept in a thermostatted shaking water bath that was maintained at 37 °C and 100 rpm. At predetermined time intervals, the release buffer was removed for analysis, and fresh PBS (with 10 mg/mL heparin) was added for continuing incubation. The amount of released pbFGF was detected with Hoechst 33258 dye as described above.

Cells and Cell Seeding on Fibrous Mats. MEFs were used to evaluate bFGF expression, and obtained as described by Joyner.[19] All animal procedures were approved by the University Animal Care and Use Committee. Briefly, pregnant mice, days 14 to 16, were from Sichuan Dashuo Biotech Inc. (Chengdu, China). Fetuses were collected aseptically at necropsy and then finely minced using microscissors. The minced tissues were washed three times with PBS free of Ca^{2+} and Mg^{2+}, and trypsinized in 0.1% trypsin/0.05% EDTA solution (Gibco BRL, Rockville, MD) while being stirred. Suspended cells were sieved through a stainless steel mesh and centrifuged at 700*g* for 5 min. The cell pellet was resuspended in Dulbecco's modified Eagle's medium (DMEM, Gibco BRL, Rockville, MD) containing 4 mM L-glutamine, 4.5 g/L glucose, 25 mM HEPES buffer, and 20% heat inactivated fetal calf serum (FCS, Gibco BRL, Grand Island, NY). The cell suspension was placed in 75 cm^2 cell culture flasks at 37 °C, 5% CO_2 in air, and the culture medium was refreshed every 3 days. After reaching 80−90% confluence, MEFs were trypsinized and the third generation from the same animal was subcultivated on fibrous mats.

Before cell seeding, 25 mm diameter disks were punched from the fibrous mats, fixed by a cell-culture ring with 22 mm of internal diameter as designed by Zhu et al.,[20] and sterilized by electron-beam irradiation using linear accelerator (Precise, Elekta, Crawley, U.K.) with a total dose of 80 cGy. A total of 200 μL of MEF suspension (2 × 10^5 cells/mL) was seeded onto the presoaked fibrous mats and placed in a 12-well tissue culture plate (TCP). The cell-seeded mats were incubated at 37 °C in a humidified atmosphere for 4 h to make cells diffuse into and adhere to the scaffold before the addition of 3.5 mL of culture medium into each well. The cell-seeded scaffolds were replenished with fresh medium every 3 days.

Characterization of Cellular Behaviors on Fibrous Mats. SEM was used to observe the morphologies of cells on fibrous mats. Briefly, samples were harvested on day 7 after seeding, washed with PBS twice, and then fixed with 4% glutaraldehyde for 2 h at 4 °C. Following three rinses with distilled water, the samples were dehydrated through a series of graded ethanol solutions, freeze-dried, and observed by SEM.

Cell viability and attachment were assayed with cell counting kit (CCK-8, Dojindo Molecular Technologies, Inc., Kumamoto, Japan). Briefly, all the fibrous mats were rinsed, moved to another 24-well TCP, and immersed into 400 μL of fresh culture medium in each well. Then 40 μL of CCK-8 reagent was added into each well and incubated for 2 h according to the reagent instruction. An aliquot (150 μL) of incubated medium was pipetted into a 96-well TCP, and the absorbance at 450 nm was measured for each well using a μQuant microplate spectrophotometer (Elx-800, Bio-Tek Instrument Inc., Winooski, VT). The cell attachment was examined 4 h after cell seeding, and the cell viability test was repeated on days 1, 3, 5, and 7 after incubation. All experiments were performed with n = 6.

Transfect Efficiency and bFGF Expression of Cells on Fibrous Mats. Expression of fusion protein bFGF/eGFP in MEFs cells was observed under a fluorescence microscope (Leica DMR HCS, Germany). Fibrous mats were harvested at predetermined time intervals after cell seeding, washed with PBS twice, fixed with 4% glutaraldehyde for 2 h at 4 °C, and then observed by the fluorescence microscope. To measure the level of gene transfection, cell loaded fibrous mats were collected at predetermined time points, washed three times with PBS, and homogenized in the lysis buffer (0.1 M Tris-HCl, 2 mM EDTA, 0.1% Triton X-100). The lysate (500 μL) was centrifuged at 12000 rpm for 5 min at 4 °C (Beckman Coulter Microfuge 22R, Altanta, GA), and the supernatant was carefully collected and kept on ice. The relative light unit (RLU) was quantified using a fluorospectrophotometer at an excitation wavelength of 493 nm and an emission wavelength of 510 nm. The total protein of the cell lysate was determined by BCA protein assay kit (Pierce, Rockford, IL). Results of GFP expression were normalized as relative light units per mg of soluble protein (RLU/mg of protein).

The target protein was quantified by the ELISA kit for bFGF (Uscn Life Science Inc., Wuhan, China) based on the manufacturer's protocol. In brief, the lysate was added into ELISA plates precoated with capture monoclonal antibodies, and detected by anti-bFGF polyclonal antibodies. Streptavidin-conjugated HRP was added to each well, followed by the addition of the enzyme substrate. After incubation for 20 min for color development, the enzyme reaction was stopped by addition of an acidic solution. The absorbance was read at 492 nm using a μQuant microplate reader. The amount of bFGF in the lysate was determined from a calibration curve based on known concentrations of bFGF.

Creation of Diabetic Skin Wound and Treatment with Fibrous Mats. Type I diabetes rat model was established as described previously.[21] Briefly, male SD rats, weighing 180 to 220 g, were from Sichuan Dashuo Biotech Inc. (Chengdu, China). Rats were given a single intraperitoneal injection of 60 mg/kg STZ dissolved in sodium citrate buffer. Whole blood was obtained 3 days later from tail vein, and the glucose level was monitored using a complete blood glucose monitor (Shenzhen Radiant Innovation CO., LTD, China). STZ-treated rats with whole-blood glucose levels higher than 16.7 mM were considered diabetic.[21] After being anesthetized with pentobarbital (45 mg/mL), the dorsal areas of diabetic rats were totally

depilated by Na_2S (8.0%, w/v) and four full-thickness circular wounds (about 250 mm^2) were created on the upper back of each mouse using a pair of sharp scissors and a scalpel.

The diabetic skin wounds were covered with Fb2 fibrous mats (11.5 mg each), polyplex infiltrated Fa2 fibrous mats (11.5 mg PELA fibrous mats soaked with 200 μL of PBS containing 1.0 μg of pbFGF polyplexes), Fa2 fibrous mats (11.5 mg each) and saline as control, respectively. Fibrous mats were sterilized before treatment, and antiseptic gauze infiltrated with ampicillin was placed as a cover over the fibrous mats and sewn to the skin around the wound area to avoid wound infection.

Evaluation of Wound Healing Process. The wound area was examined after treatment for 1, 2, 3, and 4 weeks. The skin wounds of ten animals were photographed, and the area of unhealed wound was measured based on the image using Photoshop v8.0. At weeks 1, 2, 3, and 4 after operation, 4 rats were sacrificed to retrieve trauma samples for histopathological examinations by hematoxylin−eosin (HE) staining for inflammatory reaction, cell proliferation and blood vessel formation, by SR staining for collagen secretion, and by immunohistochemical (IHC) staining of collagen type I.

HE-stained sections were observed with a Nikon Eclipse E400 light microscope (Nikon Eclipse E400, Japan). For SR staining, the cryosections were stained with hematoxylin for 8 min and SR for 1 h. The stained sections were observed with a polarized light microscope (Leica 12POLS, Germany). For IHC staining, the endogenous peroxidase was inactivated by incubation the cryosections with 3% H_2O_2 for 10 min. The antigens were recovered by putting the sections into 10 mM citrate buffer solution (pH 6.0) and heating in a microwave oven twice. Nonspecific binding sites were blocked with 5% BSA in Tris-buffered saline for 20 min, followed by incubation of the sections with primary antibodies at 4 °C overnight. Then the sections were incubated with biotinylated secondary antibody for 20 min, followed by incubation with streptavidin−HRP for 20 min. The antibody binding sites were visualized by incubation with a DAB−H_2O_2 solution. The slides were counterstained for 1 min with hematoxylin and then dehydrated with sequential ethanol for sealing and microscope observation.

Western Blot Analysis. At weeks 1, 2, 3, and 4 after treatment, 6 rats were sacrificed to collect tissues in the wound area. The tissues were homogenized in RIPA lysis buffer, and the total protein of the lysate was determined by BCA protein assay kit as above. The expressions of PCNA, CD34, collagen type I in regenerated tissue were detected by Western blot analysis with β-actin as protein loading control. Briefly, the lysate was mixed with loading buffer and then subjected to electrophoresis on 10% SDS−PAGE gel at 100 V (Power Pac Universal, Bio-RAD, Hercules, CA), followed by transfer to PVDF membrane (Millipore Corp., Bedford, MA). After being blocked with 5% BSA for 2 h at room temperature, the membrane was washed and incubated with primary antibody at a dilution of 1:1000 for 1 h at room temperature and kept at 4 °C overnight. Membranes were then washed three times with PBS containing 0.05% Tween 20 and reacted with secondary HRP-conjugated antibody for 1 h. Antigen−antibody complexes were visualized by DAB developer.

Statistics Analysis. The values were expressed as means ± standard deviation (SD). Whenever appropriate, two-tailed Student's t test was used to discern the statistical difference between groups. A probability value (p) of less than 0.05 was considered to be statistically significant.

RESULTS AND DISCUSSION

Characterization of pbFGF-Loaded Fibers. Figure 1 shows the fibrous morphology and core−sheath structure of

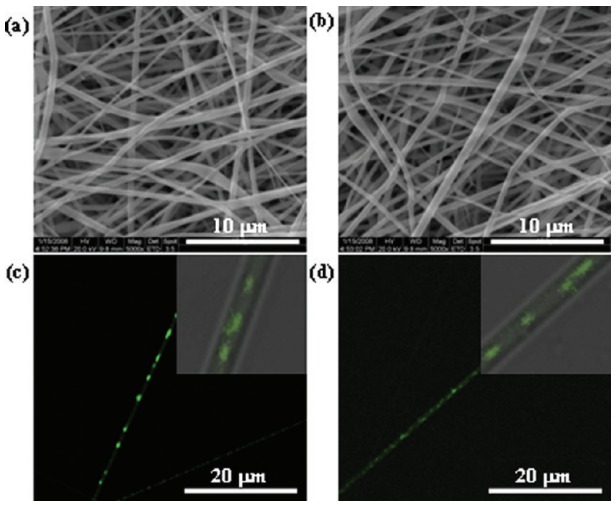

Figure 1. SEM images for (a) Fb2 and (b) Fb4 fibrous mats. LCSM images of (c) Fb2 and (d) Fb4 fibers. Insets show the images of the same fiber with and without excitation superimposed on one another.

Fb2 and Fb4 fibers. SEM images displayed a consistent fibrous structure that was bead-free, and the diameters of Fb2 and Fb4 fibers were 764 ± 327 and 822 ± 266 nm, respectively. In order to visualize the structure of the composite fibers obtained, pbFGF were labeled with DAPI, and electrospun fibers with entrapment of labeled pbFGF polyplexes were obtained. Figure 1c and Figure 1d show the CLSM images of labeled fibers with excitation, suggesting the presence of DAPI labeled polyplexes within fibers. The superimposing images of a single fiber with and without excitation on one another exhibited blue light spots in the core and a lightless outer layer, indicating a core−sheath structure of the composite fiber (insets of Figure 1c and Figure 1d). In the emulsion electrospinning process the emulsion droplets exited the capillary, and were stretched into an elliptical shape in the direction of the fiber trajectory. This inward movement of aqueous phase of the emulsion was caused by the rapid evaporation of the solvents in the oil phase. As chloroform evaporated faster than water, it was this viscosity difference between the elliptical droplets and the polymer solution that directed pDNA polyplexes to settle into the fiber interior rather than on the surface.[7]

The theoretical pbFGF loading of 0.1% (w/w) was based on an overall consideration of the *in vitro* pbFGF release rate and the preliminary tests on the transfection efficiency in our previous study.[15] Core loading efficiency of pbFGF in Fb2 and Fb4 fibers was 87.7 ± 16.5% and 79.3 ± 11.6%, respectively. The emulsion electrospinning could provide high encapsulation efficiency, and most of the pDNA loss was resulted from the formation and purification of pDNA polyplexes.[15]

***In Vitro* pbFGF Release Profiles.** The pDNA polyplexes were incorporated into electrospun fibers to enhance the transfection efficiency. Due to the size of around 200 nm and the interactions with matrix polymers, pDNA polyplexes did not diffuse appreciably in the release medium until the matrix polymers had been significantly degraded.[15] PEG was added into the fiber matrix to accelerate the release process, and the effective release time of pDNA can be modulated from 6 to 25

dx.doi.org/10.1021/mp200246b | *Mol. Pharmaceutics* 2012, 9, 48−58

days depending on the molecular weight and contents of PEG.[15] To achieve a balance between the transfection efficiency and cell viability, 10% of PEG of 2 or 4 kDa was included into the matrix polymers to allow a sustained release of pbFGF within 4 weeks, which was in accordance with the duration for skin wound recovery.

Figure 2 shows the cumulative release profiles of pbFGF from core−sheath structured fibers Fb2 and Fb4, both of which

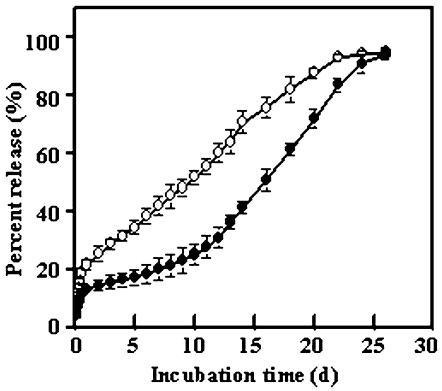

Figure 2. *In vitro* release profiles of pbFGF from Fb2 (●) and Fb4 (○) fibrous mats (n = 3).

can be described with two phases: an initial burst release followed by a sustained phase. The burst release during initial 12 h from Fb2 and Fb4 fibers was 11.8 ± 1.34% and 18.9 ± 1.55%, respectively. Although pbFGF was released out within around 26 days for both fibers, different profiles were indicated in the gradual release phase. During the initial 12 day incubation higher release rate was detected for Fb4 than Fb2 fibers. It was presumed that longer molecular chains of higher molecular weight PEG led to larger channels and faster medium exchange after dissolving. The dissolution of PEG caused microscopic holes in the fibers and increased the contact area of matrix polymer with the medium, leading to a swollen fiber matrix and accelerated degradation of matrix polymers. This may enhance the release of pbFGF from Fb2 fibers during the last 2 weeks (Figure 2). In contrast, the concentration gradient of pbFGF polyplexes between the fiber core and surface decreased due to the initial fast release from Fb4 fibers, resulting in a gradual decrease in the release rate during the last 2 weeks.

Cell Attachment and Viability on Fibrous Mats. The attachment and growth behaviors of MEFs were determined on Fb2 and Fb4 fibrous mats, compared with Fa2, Fa4 fibers and TCP with or without inclusion of pbFGF polyplexes. The attachment ability indicated the number of cells on fibrous mats with respect to those on TCP after 4 h incubation, and the results are summarized in Figure 3a−c. The cell attachment on Fa2 and Fa4 fibrous mats was significantly lower than that on TCP ($p < 0.05$), which may be due to the hydrophobic surface of electrospun fibers.[22] The cell adhesion on a surface is considered to be strongly influenced by the balance of hydrophilicity and hydrophobicity. Many studies have demonstrated that cells adhere, spread and grow more easily on moderately hydrophilic substrates than on hydrophobic or very hydrophilic ones.[23] As shown in Figure 3, an obvious inhibiting effect on the cell attachment was observed regardless of encapsulation or infiltration of pbFGF polyplexes into fibrous mats. The presence of pbFGF polyplexes indicated much remarkable cytotoxicity and suppression of cell adhesion. The amounts of burst release from polyplex-encapsulated fibers were lower than those diffused out from polyplex-infiltrated

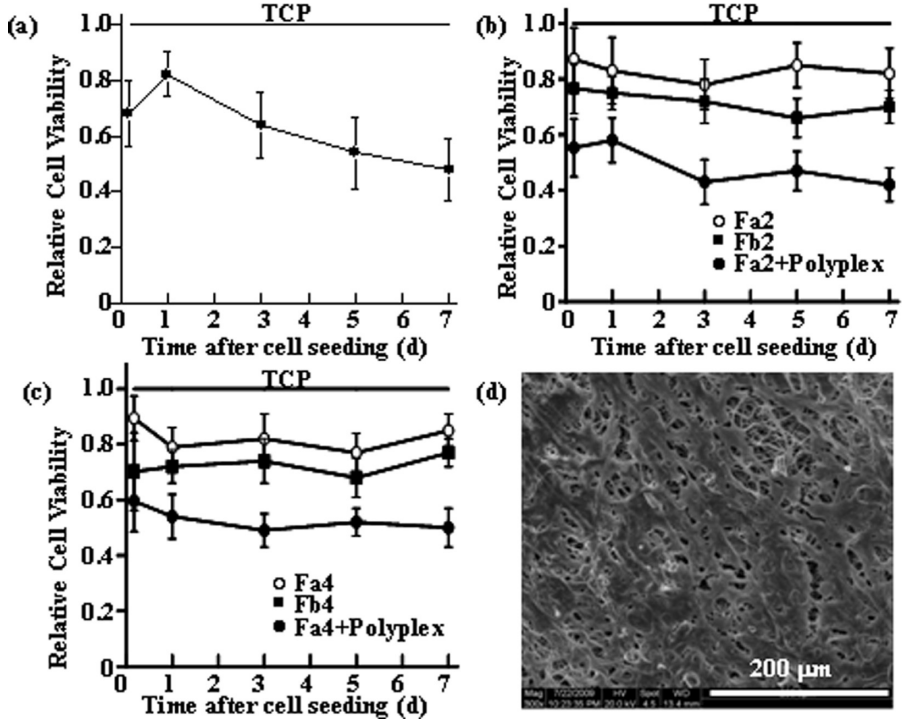

Figure 3. Cell attachment after 4 h seeding and cell viability at different time points after incubation MEFs (a) with free pbFGF polyplexes, (b) on Fb2, Fa2 fibrous mats with and without pbFGF polyplex infiltration, and (c) on Fb4, Fa4 fibrous mats with and without pbFGF polyplex infiltration, compared with TCP (solid lines) (n = 6); (d) SEM images of cell-grown Fb2 fibrous scaffolds.

dx.doi.org/10.1021/mp200246b | *Mol. Pharmaceutics* 2012, 9, 48−58

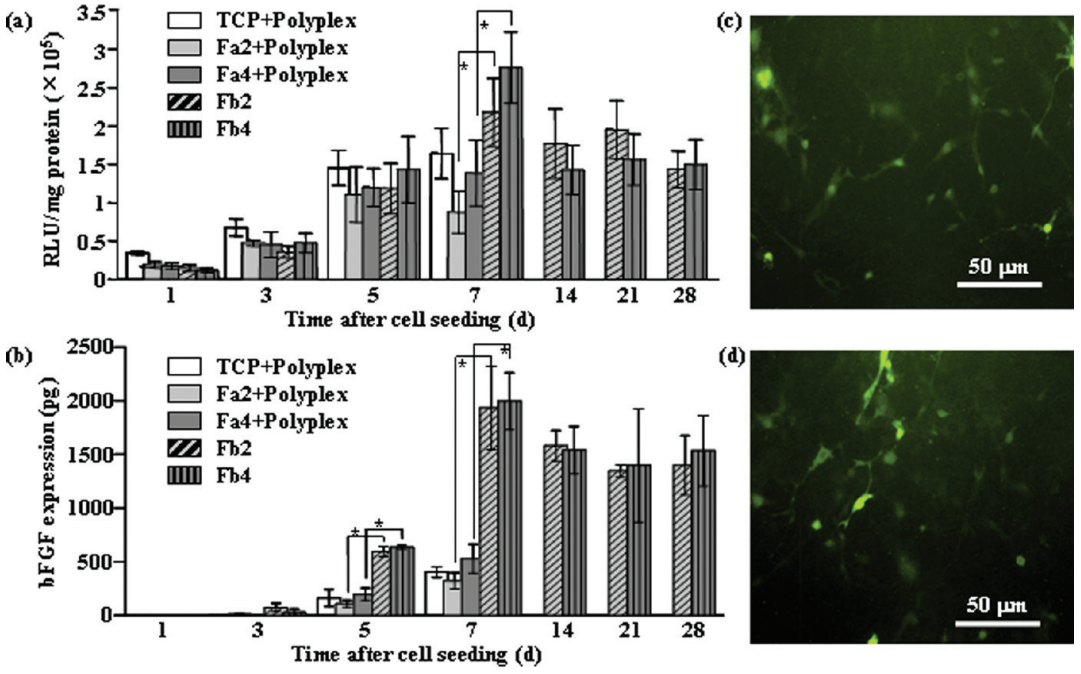

Figure 4. (a) Transfection efficiency and (b) bFGF expression of MEFs after incubation with free pbFGF polyplexes, and after being seeded on fibrous scaffolds Fb2 and Fb4, pbFGF polyplex-infiltrated fibrous scaffolds Fa2 and Fa4, compared with TCP ($n = 6$, *: $p < 0.05$). The fluorescence microscope images of bFGF/eGFP fusion protein expression on Fb2 fibrous scaffolds after (c) 7 and (d) 28 day incubation.

fibers, leading to a significantly higher cell attachment on Fb2 and Fb4 fibers ($p < 0.05$).

Figure 3a–c summarizes the cell viability on fibrous scaffolds after incubation for different time periods. The cell growth rates on all the fibrous scaffolds were similar to that on TCP. The pDNA polyplexes were detrimental to cell growth, but the expression of target protein bFGF from transfected cells by pbFGF polyplexes could promote cell proliferation. Therefore, the growth rates of cells were dependent on the competition of cytotoxicity of polyplexes and growth promotion effect of bFGF. In addition, the sustainable release of pbFGF polyplexes was supposed to keep high transfection efficiency and continuous bFGF expression, resulting in a slight increase in the growth rate during the last several days for Fb2 and Fb4 fibers (Figure 3b,c).

The cell morphology and dispersion within the fibrous mats were observed by SEM. No apparent difference was found in the morphology of cells grown and spread on the fibrous scaffolds with or without polyplex encapsulation or infiltration. Figure 3d shows the cell morphology after 7 day incubation on Fb2 fibrous mats, indicating that cells were tightly attached on the fibrous scaffold, stretched very well, and overspread nearly 70% of the scaffold surface.

Transfection Efficiency and bFGF Expression of MEFs on Fibrous Scaffolds. The recombinant plasmid of pbFGF can express fusion protein of bFGF/eGFP. Figure 4 summarizes the transfection efficiency and bFGF expression of MEFs on Fb2 and Fb4 fibrous mats, compared with Fa2, Fa4 fibers and TCP with or without inclusion of pbFGF polyplexes. As shown in Figure 4a, during the initial 5 day incubation no significant difference in the transfection efficiency was detected among the fibrous scaffolds with pbFGF polyplex infiltration or encapsulation ($p > 0.05$). However, significantly higher transfection efficiency was found for Fb2 and Fb4 fibers than polyplex infiltrated fibers after 7 day incubation ($p < 0.05$). One possible reason was the disintegration of pbFGF polyplexes in the cell culture medium, leading to a gradual decrease in the transfection efficiency with extension of time. In contrast, the gradually released polyplexes kept the intact structure and maintained the transfection capabilities. As shown in Figure 4b, the bFGF expression of MEFs on Fb2 and Fb4 fibers could be shown with the ELISA kit after 3 day culture and increased with the extension of incubation time. Significantly higher bFGF expressions were detected after 5 and 7 day incubation of MEFs on pbFGF polyplex-entrapped fibers than those on polyplex-infiltrated scaffolds ($p < 0.05$), while there was no significant difference between Fb2 and Fb4 fibers ($p > 0.05$). After 7 day incubation, the amounts of bFGF expressed on Fb2 and Fb4 fibers were 1932 ± 387 and 1995 ± 266 pg, and those of polyplex-infiltrated Fa2 and Fa4 fibers were 322 ± 76 and 529 ± 135 pg, respectively.

The gradual release of pbFGF from Fb2 and Fb4 fibers was supposed to transfect cells and enhance bFGF expression continuously. In the current study, MEFs were removed from fibrous scaffolds by trypsinization after 7 day culture, and an almost complete removal was indicated by SEM observation. Another batch of cells was seeded on the recovered fibrous mats and incubated for additional 7 days, and the cell depletion and inoculation processes were repeated until the total culture time of 28 days. As shown in Figure 4a,b, the reseeded MEFs on Fb2 and Fb4 fibers indicated remarkable transfection and bFGF expression on days 14, 21, and 28 after incubation. The amounts of bFGF expression on day 28 were 1399 ± 28 and 1533 ± 327 pg for Fb2 and Fb4 fibers, respectively. This indicated the capabilities of pDNA loaded fibrous scaffolds to extend the availability of GFs at effective levels within local tissue environment. Figure 4c and Figure 4d shows the transfected cells on Fb2 fibrous mats after 7 and 28 day incubation, both emitting green fluorescence.

Macroscopic Observation of the Wound Healing Process. As indicated above, the release profiles of pbFGF polyplexes were affected by PEG molecular weight (Figure 2),

dx.doi.org/10.1021/mp200246b | *Mol. Pharmaceutics* 2012, 9, 48–58

but *in vitro* tests on MEFs indicated that there was no significant difference between Fb2 and Fb4 fibers in the cell viability within 7 day culture (Figure 3), transfection efficiency and bFGF expression during 28 day incubation (Figure 4) ($p > 0.05$). In the following study Fb2 fibrous scaffolds were further assessed for the capabilities to promote skin regeneration. It was indicated that the pathogenic features of healing-impaired skin wounds observed in diabetic patients were well duplicated in STZ-induced diabetic rats.[24] Diabetic rats were established after 2−3 days of a single STZ injection, and the blood glucose level reached 26.4 ± 4.2 mM at day 3 after injection in current study. There was a slight decrease after feeding for a period of time, and the blood glucose level was 23.1 ± 3.7 mM by the end of tests. A series of typical clinical symptoms of diabetic mellitus arose in the experimental rats, such as polydipsia and polyuria. There was around 20% (40 g) of weight loss after the establishment of diabetic rats, and the weight gain was significantly lower during the following period compared with normal rats. Skin wounds of around 250 mm^2 were created after removal of the full-thickness skin on the back of diabetic rats, and then covered with fibrous mats as described previously.[8] The porous structure and high specific surface areas of electrospun fibrous mats allowed gaseous and fluid exchanges, absorbed excess exudates and wound odor, and closely attached to the wound surface, indicating one of the most suitable wound dressing materials.

Figure 5a shows the wound healing process after treatment with fibrous mats Fb2, Fa2 and pbFGF polyplex-infiltrated Fa2 mats, using untreated wound as control. The photographic evaluation showed that the skin wounds were healed better and faster after being treated by Fb2 fibrous mats than other groups. The shriveling of the epithelium and complete closing of the wounds were observed in Fb2 group at week 3 after operation, and the regenerated skin was smooth and similar with normal skin at week 4. A rough and thin skin layer was formed at week 4 after covering with pbFGF polyplex-infiltrated fibrous mats. However, the wounds were not closed after 4 week treatment with Fa2 fibers, and the unhealed area of the control group was much larger than that of other groups. As shown in Figure 5a, the wound repairing profiles were also different during the early healing process after treatment with the above fibrous mats for 1 week. A visible sign of healing was found in the Fb2 group with basilar membrane congestion and abundant granulation tissue surrounded with regenerated skin. Within the wounds covered with Fa2 fibrous mats with or without addition of polyplexes, local scab, marked inflammation and only thin granulation were observed. There was no scab, no infection and little granulation in the control group.

The wound images were quantified to show the unhealed areas of each experimental group at different time points. As shown in Figure 5b, the differences in the areas of unhealed wounds among the experimental groups were not significant at week 1 after operation ($p > 0.05$), but were remarkable after treatment for 2, 3, and 4 weeks ($p < 0.05$). The wounds were almost closed after 3 week treatment with Fb2 fibers, while the unhealed areas were around 13%, 22% and 33% of the initial size after treatment with polyplex-infiltrated Fa2 fibers, Fa2 fibers and control group, respectively. The faster healing of skin wounds in the Fa2 group than untreated wounds may be due to the protective effect of fibrous mats against infection and the massive degradation products of matrix polymers, which could stimulate inflammatory cell aggregation and promote the cell migration into the wound areas.[25] In addition, the sustained

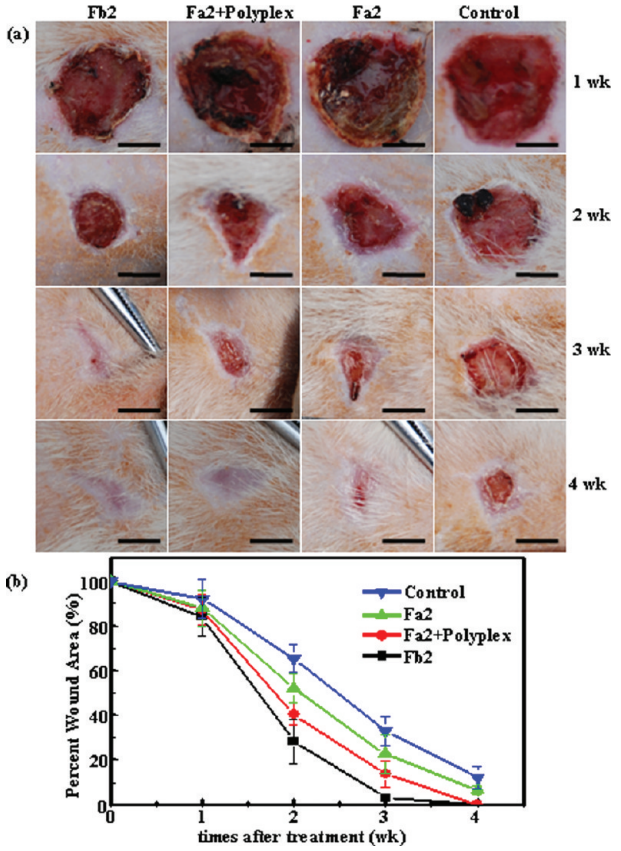

Figure 5. (a) The representative images of skin wounds after treatment with Fb2, Fa2 fibrous mats with and without pbFGF polyplex infiltration for 1, 2, 3, and 4 weeks, using untreated wound as control. Bars represent 10 mm. (b) Wound areas at different time points after treatment ($n = 10$).

release of pbFGF polyplexes from Fb2 fibers could constantly transfect cells surrounding the wound, leading to a continuous expression of bFGF to promote the migration, division and differentiation of cells for wound healing. After treatment with polyplex-infiltrated Fa2 fibrous mats pbFGF polyplexes were subjected to be removed from the wound sites due to the fluid drainage, disintegrated by the tissue fluid and deactivated by the enzymes. Thus less significant enhancement in wound healing was detected after treatment with polyplex-infiltrated mats compared with polyplex-encapsulated fibers.

Histological Observations in the Wound Area. The ultimate aim for the treatment of skin wounds is to rapidly restore the structural and functional properties to the levels of normal tissue, involving re-epithelialization and orchestrated regeneration of all the skin appendages. Re-epithelialization on the granulation tissue in open wound, forming a barrier between the wound and the environment, is one of the most important indicators for skin healing. Figure 6 shows the growth status and structure of epithelial tissue in each group at different time points. In a deep wound as in the present study, the basement membrane was breached and the skin appendages, such as hair follicles, sweat glands and sebaceous glands, were ruined. Thus the migration of epithelial cells could only occur from wound edges and on the basis of granulation tissues filling up the wound bed.[26] At week 1 after operation, the epithelial tongue could be observed in wound edges covered with Fb2 and polyplex-infiltrated Fa2 fibrous mats, indicating the climb of epithelial cells over one another in order

dx.doi.org/10.1021/mp200246b | *Mol. Pharmaceutics* 2012, 9, 48−58

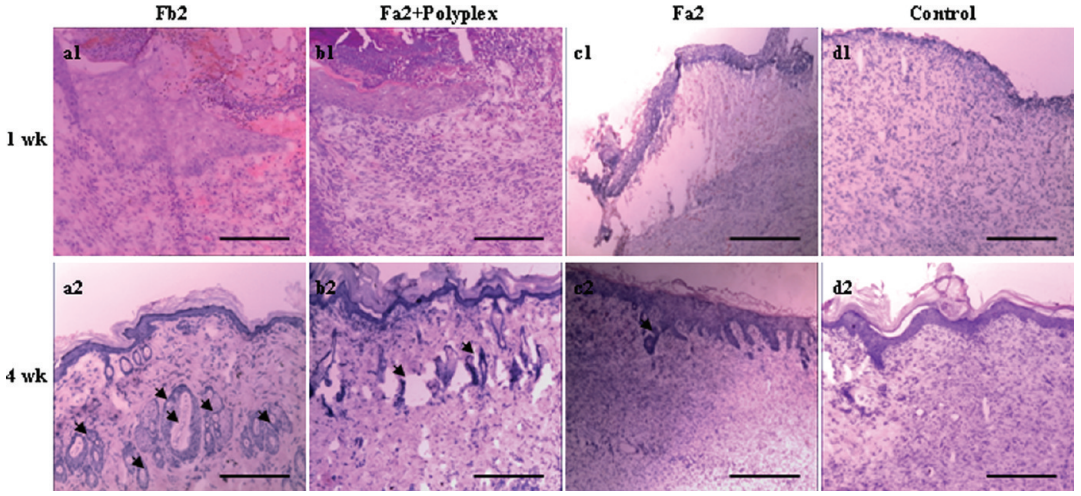

Figure 6. HE staining for re-epithelialization and formation of skin appendages in diabetic wound after treatment with Fb2, Fa2 fibrous mats with and without pbFGF polyplex infiltration for 1 and 4 weeks, using untreated wound as control. Arrows indicate hair follicles or sebaceous gland. Bars represent 200 μm.

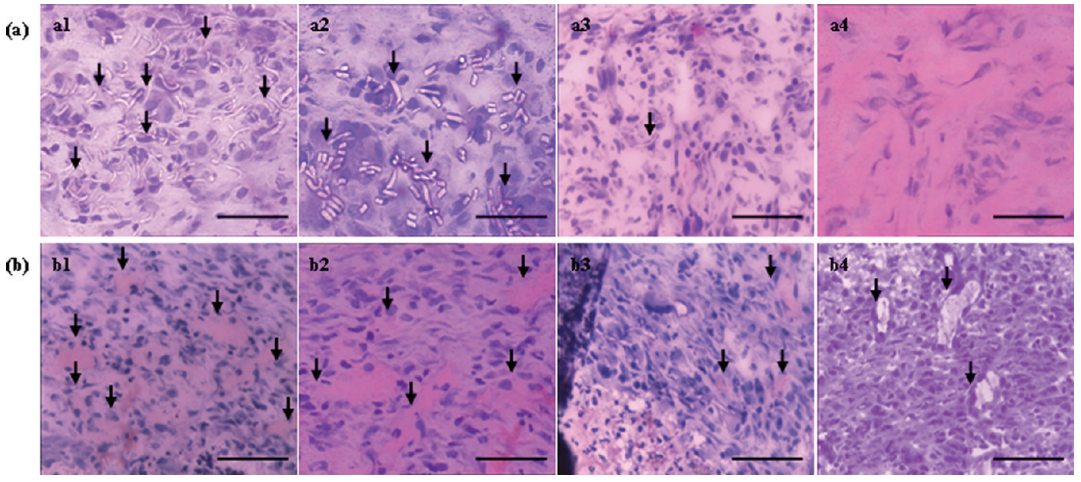

Figure 7. (a) Inflammatory reaction and fiber residuals observed by HE staining of skin wounds treated with Fb2 fibrous mats for 1 (a1), 2 (a2), 3 (a3), and 4 weeks (a4). Arrows indicate the fiber residuals. (b) HE staining for capillary vessel formation in skin wounds after 1 week treatment with Fb2 (b1), Fa2 fibrous mats with (b2) and without pbFGF polyplex infiltration (b3), using untreated wound as control (b4). Arrows indicate the capillary vessels. Bars represent 100 μm.

to migrate (Figure 6a1,b1). The more quickly this migration occurred, the less of a scar there would be.[27] In the Fa2 and control groups, the migration of epithelial cells was barely visible (Figure 6c1,d1), because of the slower growth of granulation tissue. The histological sections of the Fb2 group exhibited a spot of hair follicle cells and sebaceous gland cells at week 2 and complete re-epithelialization at week 3 after operation (data not shown). At week 4 after treatment with Fb2 fibers, the epidermic cells were fully differentiated, basal cells were closely arranged, and the horny layer and large amounts of hair and sebum could be clearly observed (Figure 6a2), indicating a similar epithelial structure with the normal skin.[8] While the wounds after treatment for 4 weeks with polyplex-infiltrated fibrous mats were also completely epithelialized but nonkeratinized (Figure 6b2), the epidermis in Fa2 and control groups was still partially unclosed (Figure 6c2,d2). The skin appendages appeared at week 4 after treatment with Fa2 fibers with and without polyplex inoculation (Figure 6b2 and c2), but were still barely visible in the control group (Figure 6d2). These results indicated that the sustained supply of pbFGF polyplexes by Fb2 fibers could transfect the cells in and around the wound and continuously express bFGF, which improved the proliferation of neonatal granulation tissue and offered optimum conditions for epithelial cell migration. The expressed bFGF can also stimulate the keratinocytes to release epidermal growth factor, which aided both in epithelialization and in other phases of wound healing.[28]

Wound healing is a complex process of tissue repair following injury, which consists of a series of coordinated overlapping biological events, involving acute and chronic inflammations, cell division, and ECM synthesis.[29] Histological studies were employed through HE staining to investigate the inflammatory reaction and the formation of blood vessels during the healing processes. All the experimental groups exhibited abundant inflammatory cells that were wound with polymeric fibers, while the control group showed inflammatory cells only at 1 week after treatment. Figure 7a shows inflammatory cells and fiber residuals in skin wounds after treatment with Fb2 fibers. After 2 weeks of operation polymeric fibers were degraded through the phagocytosis of cells and the

dx.doi.org/10.1021/mp200246b | *Mol. Pharmaceutics* 2012, 9, 48−58

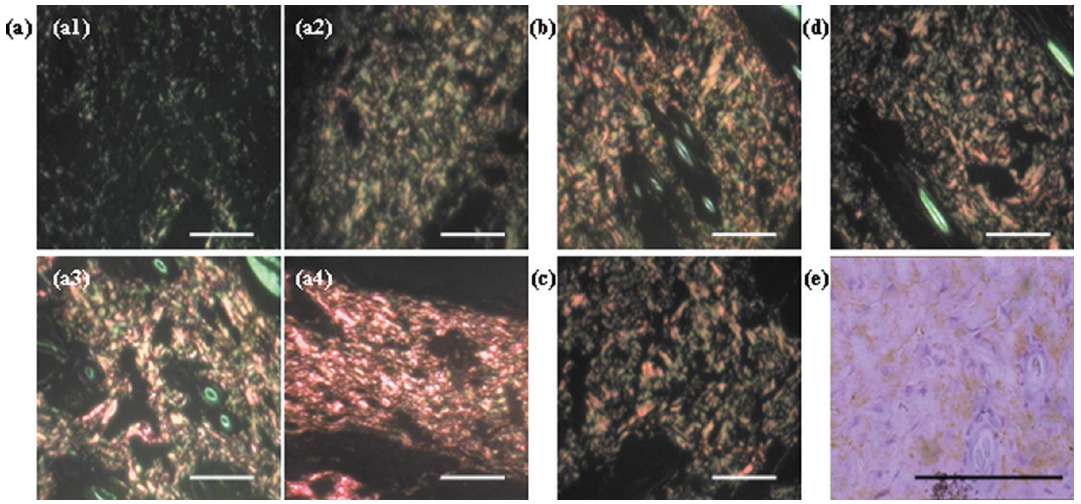

Figure 8. Polarimicroscope images of SR staining of skin wounds treated with (a) Fb2 for 1 (a1), 2 (a2), 3 (a3), and 4 weeks (a4), and Fa2 fibrous mats (b) with or (c) without pbFGF polyplex infiltration for 4 weeks, using untreated wound at week 4 as control (d). (e) Immunohistochemical staining image for collagen I expression in skin wounds treated with Fb2 fibrous mats for 4 weeks. Bars represent 200 μm.

invasion of tissue fluids, and there were very tiny amounts of fiber residue being observed in the histological sections at week 3. It was indicated that the fiber loss is significantly higher than *in vitro* incubation in PBS.[30] Meanwhile, remarkable ECM secretion was found in the extracellular space, and the histological sections of the Fb2 group showed similar structure with normal skin 4 weeks after operation (Figure 7a4).

Angiogenesis is imperative in wound healing to maintain the cell activity for tissue repair, and precursor cells present within the blood should migrate to sites of injury though the high density of blood vessels to mediate the skin regeneration. The tissues in all the skin wounds looked red 1 week after operation, due to the presence of capillaries. Figure 7b shows HE staining for capillary vessel formation in wound skin after 1 week treatment, indicating a higher blood vessel density in fibrous group than control. We speculated that these differences were primarily due to the different states of hypoxic environment and acid degradation products of fiber matrices.[31] The inflammatory response induced by fiber degradation could stimulate the endothelial cells, originated from parts of uninjured blood vessels, to develop pseudopodia and migrate into the wound site to establish new blood vessels.[32] The bFGF expression should promote the endothelial growth and proliferation as its mitogenic effect.[33] On the other hand, the cell growth and proliferation led to a high metabolic rate and low oxygen content in the regenerated tissues, which were supposed to promote vasculogenesis.[31] In addition, when tissue was adequately perfused, numerous cells in the wound area were no longer in the hypoxic and acidic environment, and thus the migration and proliferation of endothelial cells were reduced. Therefore, with the extension of wound healing time, microvessels in histological sections of each experimental group became gradually less until little remained.

Collagen Secretion in the Wound Healing Process. Collagen fiber is the framework of dermis, and a healing wound is mainly a result of the net deposition and stabilization of collagen in the wound area. Cells involved in inflammation, angiogenesis, and connective tissue construction attach to, grow and differentiate on the collagen matrix.[34] As shown in the HE staining results of wound skin (Figure 7), collagen deposition was observed in the Fb2 group at week 2 after treatment. With the prolongation of wound healing, the inflammatory cells and microvessels in the regenerated tissues were gradually degraded and substituted by collagen fibers, and remarkable content of collagen was detected at week 4 after treatment. Besides this, the type of collagen fibers is considered to be a key point of keloids and hypertrophic scar formation.[35] Therefore, SR and IHC staining were applied in the present study to analysis the collagen deposition and remolding in the regenerated tissues.

Figure 8 shows the polarimicroscopic images of collagen fibers by SR staining, where the red area denotes collagen type I and green denotes collagen type III. A small amount of collagen type III was observed in the Fb2 group at week 1 after operation (Figure 8a1), and the wound area was filled with collagen production after 3 week treatment (Figure 8a3). Collagen type III, which was prevalent during proliferation, was gradually replaced by collagen type I during the maturation phase of tissue repair.[32] At week 4 after operation, the regenerated tissue in the Fb2 group consisted chiefly of collagen type I, with a small amount of collagen type III interspersed (Figure 8a4), which was close to the SR staining profile of normal skin.[8] As shown in Figure 8, the green area representing collagen type III was dominated in the wound skin after treatment with Fa2 fibers with and without polyplex infiltration, indicating that the collagen deposition rate and the ratio of collagen type III to type I were much lower than those of the Fb2 group. Figure 8e shows the IHC staining results of collagen type I secreted in the Fb2 group, showing that type I collagen was the main ingredient in the regenerated skin.

It is known that hypertrophic scarring, which usually occurs after deep injury of the skin, is mainly caused by excessive collagen production by fibroblasts.[36] Attempts have been made to modulate the apoptosis of fibroblastic cells to improve scar quality and balance the ECM synthesis and degradation.[37] Ono et al. demonstrated that bFGF promoted apoptosis of fibroblastic cells, leading to a reduction in wound contraction.[38] In the current study, the gradual release of pbFGF polyplexes resulted in the availability of bFGF in the later phase of the wound healing process, which was essential to modulate the cell growth and matrix remodeling. The above results indicated that the collagen production and remodeling were promoted by the continuous introduction of pbFGF polyplexes into the wound

dx.doi.org/10.1021/mp200246b | *Mol. Pharmaceutics* 2012, 9, 48–58

bed to impel the regenerated skin to possess similar collagen filling with normal skin.

Protein Expression in the Wound Healing Process. Figure 9 shows the expression of CD34, PCNA, and collagen type I in regenerated tissues by Western blotting at different time points after operation, with β-actin as protein loading control. The PCNA expression, as marker of cell proliferation, was high at week 1 after treatment with fibrous mats and invisible at week 2. The CD34 expression, as marker of vascular endothelial cells, was highest in wound skin after 1 week treatment with Fb2 fibers among the experimental groups, which was also reflected in the HE staining results as shown in Figure 7b. The expression of collagen type I in wound skin was detected at week 2 after treatment by Fb2 and pbFGF polyplex-infiltrated Fa2 fibrous mats, but no expression was found in Fa2 and control groups. The collagen expression increased quickly with healing time prolongation, and the expression level of collagen type I in the Fb2 group was much higher than in the other groups at each time point. These results were accordant with the appearances in histological sections (Figure 8), indicating that the sustained release of pbFGF polyplexes from fibrous mats led to continuous cell transfection, bFGF expression, and wound healing acceleration.

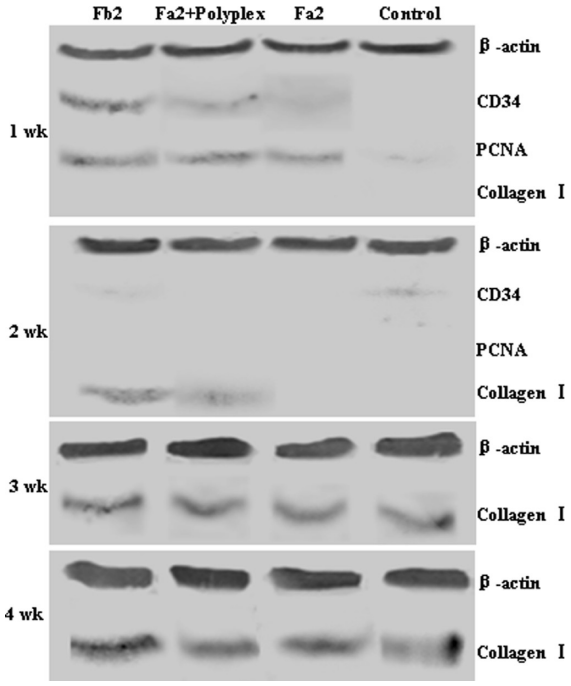

Figure 9. Western blotting assay for CD34, PCNA, and collagen expressions in skin wounds treated with Fb2, Fa2 fibrous mats with or without pbFGF polyplex infiltration for 1, 2, 3, and 4 weeks, using untreated wound as control. Total proteins were prepared from skin wounds, and β-actin expression was used as protein loading control.

CONCLUSIONS

The pbFGF polyplexes were incorporated into electrospun fibers with a core−sheath structure, and indicated a sustained release for 4 weeks, which was in accordance with the duration for skin wound recovery. Although the release profiles of pbFGF polyplexes were affected by PEG molecular weight, nevertheless *in vitro* tests on MEFs indicated that there was no significant difference between Fb2 and Fb4 fibers in the cell viability within 7 day culture, transfection efficiency and bFGF expression during 28 day incubation. *In vivo* tests on the dorsal wounds of diabetic rats showed that the gradual release of pbFGF polyplexes revealed significantly higher wound recovery rate with collagen deposition and maturation, complete re-epithelialization and skin appendage regeneration. These findings suggest the potential use of pbFGF-loaded electrospun fibrous mats to rapidly restore the structural and functional properties of wounded skin for patients with diabetes mellitus.

AUTHOR INFORMATION

Corresponding Author

*School of Materials Science and Engineering, Southwest Jiaotong University, Chengdu 610031, P. R. China. Phone: +8628-87634068. Fax: +8628-87634649. E-mail: xhli@swjtu.edu.cn.

ACKNOWLEDGMENTS

This work was supported by National Natural Science Foundation of China (20774075 and 51073130), National Basic Research Program of China (973 Program, 2012CB933602) and Fundamental Research Funds for the Central Universities (SWJTU11CX126, SWJTU11ZT10, and SWJTU09ZT21).

REFERENCES

(1) Yannas, I. V.; Kwan, M. D.; Longaker, M. T. Early fetal healing as a model for adult organ regeneration. *Tissue Eng.* **2007**, *13*, 1789−1798.

(2) Ishihara, M.; Nakanishi, K.; Ono, K.; Sato, M.; Saito, Y.; Yura, H.; Matsui, T.; Hattori, H.; Uenoyama, M.; Kikuchi, M.; Kurita, A. Photocrosslinkable chitosan as a dressing for wound occlusion and accelerator in healing process. *Biomaterials* **2002**, *23*, 833−840.

(3) Nagato, H.; Umebayashi, Y.; Wako, M.; Tabata, Y.; Manabe, M. Collagen-poly(glycolic acid) hybrid matrix with basic fibroblast growth factor accelerated angiogenesis and granulation tissue formation in diabetic mice. *J. Dermatol.* **2006**, *33*, 670−675.

(4) Greiner, A.; Wendorff, J. H. Electrospinning: a fascinating method for the preparation of ultrathin fibers. *Angew. Chem., Int. Ed.* **2007**, *46*, 5670−5673.

(5) Yoo, H. S.; Kim, T. G.; Park, T. G. Surface-functionalized electrospun nanofibers for tissue engineering and drug delivery. *Adv. Drug Delivery Rev.* **2009**, *61*, 1033−1042.

(6) Jiang, H.; Hu, Y.; Li, Y.; Zhao, P.; Zhu, K.; Chen, W. A facile technique to prepare biodegradable coaxial electrospun nanofibers for controlled release of bioactive agents. *J. Controlled Release* **2005**, *108*, 237−243.

(7) Yang, Y.; Li, X.; Qi, M.; Zhou, S.; Weng, J. Release pattern and structural integrity of lysozyme encapsulated in core−sheath structured poly(DL-lactide) ultrafine fibers prepared by emulsion electrospinning. *Eur. J. Pharm. Biopharm.* **2008**, *69*, 106−116.

(8) Yang, Y.; Xia, T.; Zhi, W.; Wei, L.; Weng, J.; Zhang, C.; Li, X. H. Promotion of skin regeneration in diabetic rats by electrospun core-sheath fibers loaded with basic fibroblast growth factor. *Biomaterials* **2011**, *32*, 4243−4254.

(9) Hadjiargyrou, M.; Chiu, J. B. Enhanced composite electrospun nanofiber scaffolds for use in drug delivery. *Expert Opin. Drug Delivery* **2008**, *5*, 1093−1106.

(10) Luu, Y. K.; Kim, K.; Hsiao, B. S.; Chu, B.; Hadjiargyrou, M. Development of a nanostructured DNA delivery scaffold via electrospinning of PLGA and block copolymers. *J. Controlled Release* **2003**, *89*, 341−353.

(11) Sakai, S.; Yamada, Y.; Yamaguchi, T.; Ciach, T.; Kawakami, K. Surface immobilization of poly(ethyleneimine) and plasmid DNA on electrospun poly(L-lactic acid) fibrous mats using a layer-by-layer

approach for gene delivery. *J. Biomed. Mater. Res. A* **2009**, *88*, 281−287.
(12) Saraf, A.; Baggett, L. S.; Raphael, R. M.; Kasper, F. K.; Mikos, A. G. Regulated non-viral gene delivery from coaxial electrospun fiber mesh scaffolds. *J. Controlled Release* **2010**, *143*, 95−103.
(13) Nie, H.; Wang, C. H. Fabrication and characterization of PLGA/HAp composite scaffolds for delivery of BMP-2 plasmid DNA. *J. Controlled Release* **2007**, *120*, 111−121.
(14) Liang, D.; Luu, Y. K.; Kim, K.; Hsiao, B. S.; Hadjiargyrou, M.; Chu, B. In vitro non-viral gene delivery with nanofibrous scaffolds. *Nucleic Acids Res.* **2005**, *33*, 170−177.
(15) Yang, Y.; Li, X. H.; Cheng, L.; He, S. H.; Zou, J.; Chen, F.; Zhang, Z. B. Core-sheath-structured fibers with pDNA polyplex loadings for optimal release profile and transfection efficiency as potential tissue engineering scaffolds. *Acta Biomater.* **2011**, *7*, 2533−2543.
(16) Martin, C.; Robson, M. C. The role of growth factors in the healing of chronic wounds. *Wound Repair Regen.* **1997**, *5*, 12−17.
(17) Alberts, B.; Johnson, A.; Lewis, J.; Raff, M.; Roberts, K.; Walter, P. *Molecular Biology of the Cell*, 4th ed.; Garland Science Press: New York, 2006; pp 1431−1463.
(18) Deng, X. M.; Li, X. H.; Huang, Z. T.; Jia, W. X.; Zhang., Y. H. Optimization of preparative parameters for poly-DL-lactide-poly(ethylene glycol) microspheres with entrapped Vibrio cholera antigens. *J. Controlled Release* **1999**, *58*, 123−131.
(19) Joyner, A. L. *Gene Targeting: A Practical Approach*, 2nd ed.; Oxford Univ. Press: Oxford, U.K., 1993; pp 36−39.
(20) Zhu, X. L.; Cui, W. G.; Li, X. H.; Jin, Y. Electrospun fibrous mats with high porosity as potential scaffolds for skin tissue engineering. *Biomacromolecules* **2008**, *9*, 1795−1801.
(21) Wang, W.; Lin, S. Q.; Xiao, Y. C.; Huang, Y. D.; Tan, Y.; Cai, L.; Li, X. K. Acceleration of diabetic wound healing with chitosan-crosslinked collagen sponge containing recombinant human acidic fibroblast growth factor in healing-impaired STZ diabetic rats. *Life Sci.* **2008**, *82*, 190−204.
(22) Cui, W. G.; Li, X. H.; Zhou, S. B.; Weng, J. Degradation patterns and surface wettability of electrospun fibrous mats. *Polym. Degrad. Stab.* **2008**, *93*, 731−738.
(23) Arima, Y.; Iwata, H. Effect of wettability and surface functional groups on protein adsorption and cell adhesion using well-defined mixed self-assembled monolayers. *Biomaterials* **2007**, *28*, 3074−3082.
(24) Blakytny, R.; Jude, E. The molecular biology of chronic wounds and delayed healing in diabetes. *Diabetic Med.* **2006**, *23*, 594−608.
(25) Wilgus, T. A. Immune cells in the healing skin wound: influential players at each stage of repair. *Pharmacol. Res.* **2008**, *58*, 112−126.
(26) Falanga, V. The chronic wound: impaired healing and solutions in the context of wound bed preparation. *Blood Cell. Mol. Dis.* **2004**, *32*, 88−94.
(27) Son, H. J.; Bae, H. C.; Kim, H. J.; Lee, D. H.; Han, D. W; Park, J. C.; Park, J. Effects of β-glucan on proliferation and migration of fibroblasts. *Curr. Appl. Phys.* **2005**, *5*, 468−471.
(28) Bayram, Y.; Deveci, M.; Imirzalioglu, N.; Soysal, Y.; Sengezer, M. The cell based dressing with living allogenic keratinocytes in the treatment of foot ulcers: a case study. *Br. J. Plast. Surg.* **2005**, *58*, 988−996.
(29) Bryan, D.; Walker, K. B.; Ferguson, M.; Thorpe, R. Cytokine gene expression in a murine wound healing model. *Cytokine* **2005**, *31*, 429−438.
(30) Yang, Y.; Li, X. H.; He, S. H.; Cheng, L.; Chen, F.; Zhou, S. B.; Weng, J. Biodegradable ultrafine fibers with core-sheath structures for protein delivery and its optimization. *Polym. Adv. Technol.* **2010**, DOI: 10.1002/pat.1681.
(31) Kondo, T.; Ishida, Y. Molecular pathology of wound healing. *Forensic Sci. Int.* **2010**, *203*, 93−98.
(32) Greenhalgh, D. G. The role of apoptosis in wound healing. *Int. J. Biochem. Cell Biol.* **1998**, *30*, 1019−1030.
(33) Kawai, K.; Suzuki, S.; Tabata, Y.; Ikada, Y.; Nishimura, Y. Accelerated tissue regeneration through incorporation of basic fibroblast growth factor-impregnated gelatin microspheres into artificial dermis. *Biomaterials* **2000**, *21*, 489−499.
(34) Ruszczak, Z. Effect of collagen matrices on dermal wound healing. *Adv. Drug Delivery Rev.* **2003**, *55*, 1595−1611.
(35) Lu, W. W.; Ip, W. Y.; Jing, W. M.; Holmes, A. D.; Chow, S. P. Biomechanical properties of thin skin flap after basic fibroblast growth factor (bFGF) administration. *Br. J. Plast. Surg.* **2000**, *53*, 225−229.
(36) Wang, X. Q.; Liu, Y. K.; Qing, C.; Lu, S. L. Hyperactivity of fibroblasts and functional regression of endothelial cells contribute to microvessel occlusion in hypertrophic scarring. *Microvasc. Res.* **2009**, *77*, 204−211.
(37) Xie, J. L.; Bian, H. N.; Qi, S. H.; Chen, H. D.; Li, H. D.; Xu, Y. B.; Li, T. Z.; Liu, X. S.; Liang, H. Z.; Xin, B. R.; Huan, Y. Basic fibroblast growth factor (bFGF) alleviates the scar of the rabbit ear model in wound healing. *Wound Repair Regen.* **2008**, *16*, 576−581.
(38) Ono, I.; Akasaka, Y.; Kikuchi, R.; Sakemoto, A.; Kamiya, T.; Yamashita, T.; Jimbow, K. Basic fibroblast growth factor reduces scar formation in acute incisional wounds. *Wound Repair Regen.* **2007**, *15*, 617−623.